

Electromagnetic ion-cyclotron instability in a dusty plasma with product-bi-kappa distributions for the plasma particles

M. S. dos Santos,¹ L. F. Ziebell and R. Gaelzer

Instituto de Física, Universidade Federal do Rio Grande do Sul, 91501-970, Porto Alegre, RS, Brasil

michel.santos@iffarroupilha.edu.br, luiz.ziebell@ufrgs.br, rudi.gaelzer@ufrgs.br

ABSTRACT

We study the dispersion relation for parallel propagating ion-cyclotron (IC) waves in a dusty plasma, considering that ions and electrons may be represented by product-bi-kappa (PBK) velocity distributions. The results obtained by numerical solution of the dispersion relation, in a case with isotropic Maxwellian distributions for electrons and PBK distribution for ions, show the occurrence of the electromagnetic ion-cyclotron instability (EMIC), and show that the decrease in the kappa indexes of the PBK ion distribution leads to significant increase of the instability, in magnitude of the growth rates and in range in wavenumber space. On the other hand, for anisotropic Maxwellian distribution for ions and PBK distribution for electrons, the decrease of the kappa index in the PBK electron distribution contributes to reduce the EMIC instability, but the reduction effect is much less pronounced than that obtained with the same combination of distributions in the case of the ion-firehose instability, shown in a recent publication. The results obtained also show that, as a general rule, the presence of a dust population contributes to reduce the instability in magnitude of the growth rates and range, but that in the case of PBK ion distribution with small kappa indexes the instability may continue to occur for dust populations which would eliminate completely the instability in the case of bi-Maxwellian ion distributions. It has also been seen that the anisotropy due to the kappa indexes in the ion PBK distribution is not so efficient in producing the EMIC instability as the ratio of perpendicular and parallel ion temperatures, for equivalent value of the effective temperature.

1. Introduction

A recent paper has discussed the dispersion relation and the growth or damping rates of low frequency electromagnetic waves pertaining to the whistler branch, propagating along an ambient magnetic field, in a plasma in which electrons and ions can be described by product-bi-kappa (PBK) distributions, and which may contain a small population of dust particles (dos Santos et al. 2016). The growth of the low-frequency waves in this branch of the dispersion curves constitute the so-called ion-firehose instability. It may occur when there is anisotropy in the velocity distribution of the ions, caused either by anisotropy between per-

pendicular and parallel ion temperatures (namely, $T_{i\perp} < T_{i\parallel}$), or by anisotropy between the perpendicular and parallel kappa indexes which characterize a ion PBK distribution. The work done in dos Santos et al. (2016) was closely related to the work done in two other relatively recent papers dedicated to low frequency electromagnetic waves, which respectively discussed the ion-firehose instability (dos Santos et al. 2014) and the EMIC instability (which occurs when $T_{i\perp} > T_{i\parallel}$) (dos Santos et al. 2015), in a plasma without dust. One of the motivations for these studies has been the fact that observations have consistently shown that ions as well as electrons in the solar wind may have non thermal velocity distributions which feature characteristic power-law tails (Pilipp et al. 1987a,b; Maksimovic et al. 1997, 2005; Marsch et al. 2004; Marsch 2006; Hapgood et al. 2011). These distributions with power-law tails can be

¹Present address: Instituto Federal de Educação, Ciência e Tecnologia Farroupilha, 98590-000, Santo Augusto, RS, Brasil

mathematically described by functions which are generically known as kappa distributions, whose introduction for the description of velocity distributions in space environments is usually attributed to [Vasyliunas \(1968\)](#). Two different basic forms of kappa distributions are used in the literature, which are the kappa distribution as defined in [Summers and Thorne \(1991\)](#) and the kappa distribution as defined in [Leubner \(2002\)](#). Anisotropic forms of kappa distributions can also be defined, either based upon the functions defined in [Summers and Thorne \(1991\)](#) or based upon the functions defined in [Leubner \(2002\)](#), and may be useful for the discussion of instabilities in space environments. These anisotropic forms of kappa distributions are usually known as bi-kappa (BK) distributions, when feature isotropic kappa index and temperature anisotropy, or as product-bi-kappa (PBK) distributions, when the anisotropy may also occur in the kappa indexes. Another form of anisotropic kappa distribution is the kappa-Maxwellian distribution, characterized by a kappa form along parallel direction and a Maxwellian distribution along perpendicular directions ([Hellberg and Mace 2002](#); [Cattaert et al. 2007](#)). Kappa distributions, either for ions or for electrons, isotropic or anisotropic, may lead to significant modifications in the dispersion relations of electromagnetic waves and on the growth rates of instabilities in plasmas ([Pierrard and Lazar 2010](#); [Lazar and Poedts 2009a,b](#); [Lazar et al. 2011](#); [Lazar 2012](#); [Lazar et al. 2012](#); [Lazar and Poedts 2014](#); [Lazar et al. 2015](#); [dos Santos et al. 2014, 2015](#)). Bi-kappa distributions have been used, for instance, as part of tools to modelate observed features of plasmas in the Jupiter environment ([Moncuquet et al. 2002](#); [Andre and Ferriere 2008](#); [Imai et al. 2015](#)). Product-bi-kappa distributions are more flexible than bi-Maxwellians and BK distributions, since their non thermal features can be modeled by anisotropic temperatures and by anisotropic kappa indexes, and have already been used as a modeling tool in [Lazar et al. \(2012\)](#), and also in a discussion about the instability limits for the Weibel instability, in [Lazar et al. \(2010\)](#). We are not aware of other uses of PBK distributions to actually fit results of observations, but it is conceivable that they can replace with advantage the less flexible BK distributions or the combinations of bi-Maxwellians which have been used in past

data analysis. It is therefore useful to investigate the effect of PBK distributions on waves and instabilities, in order to understand the differences between wave properties in the presence of PBK distributions and in the presence of BK or bi-Maxwellian distributions.

In addition to taking into account the presence of PBK velocity distributions, [dos Santos et al. \(2016\)](#) also took into account the possibility of presence of dust in the plasma, motivated by observations which have shown that the plasma in the solar wind may contain a dust population ([Mann et al. 2004](#); [Marsch 2006](#); [Schwenn 2006](#); [Mann 2008](#); [Kruger et al. 2007](#); [Grün et al. 1985](#); [Ishimoto and Mann 1998](#); [Meyer-Vernet et al. 2009](#); [Mann 2010](#); [Krueger et al. 2015](#)). In fact, observations of the inner region of the solar system, made with satellites like Ulysses, Galileo, or Cassini, have shown the existence of a population of small dust particles, with sizes which range from the nanometric to the micrometric size. The number density of dust particles has been seen to be much smaller than that of the solar wind particles, but it is estimated that the total mass of dust particles in the inner region of the solar system may be about the same order of magnitude as the mass of plasma particles. Dust has also been observed as a significant element in some specific environments, like in the neighborhood of comets ([Mendis and Horányi 2013](#)), in planetary rings ([Goertz 1989](#)), and in the vicinity of Jupiter’s satellites ([Grün et al. 1997](#)). Dust may therefore play relevant role in the dynamics of plasma in the solar wind. The presence of dust affects the dispersion properties of plasmas, leading to modifications in the properties of plasma waves in comparison with those in a dustless plasma, and also to the occurrence of new modes, associated to the dynamics of the dust ([Shukla 1992](#); [Rao 1993](#)).

In the present paper we return to the study of effects due to the ion distribution function, particularly the effect of PBK distributions, considering now waves in the IC branch of the dispersion relation of low frequency electromagnetic wave, in a dusty plasma. The investigation is complementary to that appearing in [dos Santos et al. \(2016\)](#), which considered waves in the whistler branch, and to that appearing in [dos Santos et al. \(2015\)](#), which studied IC waves in a dustless plasma.

The paper is organized as follows: In section

2 we briefly describe the theoretical formulation which leads to the dispersion relation for electromagnetic waves propagating parallel to the ambient magnetic field in a dusty plasma, considering different forms of the velocity distribution for plasma particles, either PBK or bi-Maxwellian. The discussion which is presented is very brief and dedicated to the presentation and definition of quantities and expressions used in the present paper, with references to the literature in regard to details of the derivation. Section 3 is dedicated to presentation and discussion of results obtained by numerical solution of the dispersion relation, considering different combinations of ion and electron distribution functions and different sets of parameters. Section 4 presents some final remarks.

2. Theoretical Formulation

For electromagnetic waves which propagate along the ambient magnetic field, in plasmas with particles described by distribution functions which have even dependence on the velocity variable which is parallel to the direction of the magnetic field, the dispersion relation is obtained as the solution of the following determinant,

$$\det \begin{pmatrix} \varepsilon_{xx} - N_{\parallel}^2 & \varepsilon_{xy} & 0 \\ -\varepsilon_{xy} & \varepsilon_{xx} - N_{\parallel}^2 & 0 \\ 0 & 0 & \varepsilon_{zz} \end{pmatrix} = 0, \quad (1)$$

where it has been taken into account that, for $k_{\perp} \rightarrow 0$, $\varepsilon_{yy} = \varepsilon_{xx}$ and $\varepsilon_{xz} = \varepsilon_{yz} = 0$, and where N_{\parallel} is the parallel component of the refraction vector, $\mathbf{N} = c\mathbf{k}/\omega$.

The determinant given by equation (1) can be separated into two minor determinants, and the dispersion relation becomes the following,

$$N_{\parallel}^2 = \varepsilon_{xx} \pm i\varepsilon_{xy}, \quad (2)$$

The components of the dielectric tensor which appear in dispersion relation (2) in a dusty plasma can be written as follows

$$\begin{aligned} \varepsilon_{xx} &= 1 + \frac{1}{z^2} \sum_{\beta} \frac{\omega_{p\beta}^2}{\Omega_i^2} \frac{1}{n_{\beta 0}} \sum_{m=1}^{\infty} \left(\frac{q_{\perp}}{r_{\beta}} \right)^{2(m-1)} \\ &\times \sum_{n=-m}^m n^2 A(|n|, m - |n|) J(n, m, 0; f_{\beta 0}) \\ \varepsilon_{xy} &= -\varepsilon_{yx} = i \frac{1}{z^2} \sum_{\beta} \frac{\omega_{p\beta}^2}{\Omega_i^2} \frac{1}{n_{\beta 0}} \sum_{m=1}^{\infty} \left(\frac{q_{\perp}}{r_{\beta}} \right)^{2(m-1)} \end{aligned} \quad (3)$$

$$\begin{aligned} &\times \sum_{n=-m}^m mn A(|n|, m - |n|) J(n, m, 0; f_{\beta 0}) \\ \varepsilon_{yy} &= 1 + \frac{1}{z^2} \sum_{\beta} \frac{\omega_{p\beta}^2}{\Omega_i^2} \frac{1}{n_{\beta 0}} \sum_{m=1}^{\infty} \left(\frac{q_{\perp}}{r_{\beta}} \right)^{2(m-1)} \\ &\times \sum_{n=-m}^m B(|n|, m - |n|) J(n, m, 0; f_{\beta 0}), \end{aligned}$$

where

$$\begin{aligned} J(n, m, h; f_{\beta 0}) &\equiv z \int d^3u \frac{u_{\parallel}^h u_{\perp}^{2(m-1)} u_{\perp}}{z - nr_{\beta} - q_{\parallel} u_{\parallel} + i\tilde{\nu}_{\beta d}^0(u)} \\ &\times \left[\left(1 - \frac{q_{\parallel}}{z} u_{\parallel} \right) \frac{\partial f_{\beta 0}}{\partial u_{\perp}} + \frac{q_{\parallel}}{z} u_{\perp} \frac{\partial f_{\beta 0}}{\partial u_{\parallel}} \right] \end{aligned}$$

and where $A(n, m)$ and $B(n, m)$ are numerical coefficients. In equations 3, non dimensional variables have been used, defined $z = \omega/\Omega_i$, $r_{\beta} = \Omega_{\beta}/\Omega_i$, $\tilde{\nu}_{\beta d}^0(u) = \nu_{\beta d}^0(u)/\Omega_i$, $q_{\perp} = k_{\perp} v_A/\Omega_i$, $q_{\parallel} = k_{\parallel} v_A/\Omega_i$, $\mathbf{u} = \mathbf{v}/v_A$. The quantity $\omega_{p\beta} = \sqrt{4\pi n_{\beta 0} q_{\beta}^2/m_{\beta}}$ is the plasma frequency for species β , $\Omega_{\beta} = q_{\beta} B_0/(m_{\beta} c)$ is the cyclotron angular frequency for species β , $v_A = B_0/\sqrt{4\pi n_{i0} m_i}$ is the Alfvén velocity, and $\nu_{\beta d}^0(u)$ is the frequency of inelastic collisions between dust particles and plasma particles of species β . In terms of non dimensional variables, the frequency of inelastic dust-plasma collisions may be written as follows,

$$\begin{aligned} \nu_{\beta 0}^{j0}(u) &= \frac{\pi a_j^2 n_{d0}^j v_A}{u} \left(u^2 - \frac{2q_{d0} q_{\beta}}{m_{\beta} v_A^2 a} \right) \\ &\times H \left(u^2 - \frac{2q_{d0} q_{\beta}}{m_{\beta} v_A^2 a} \right), \end{aligned} \quad (4)$$

where q_{d0} is the equilibrium value of the dust charge. It is assumed that the dust charge is acquired via inelastic collisions between plasma particles and the dust grains, and it is therefore convenient to write $q_{d0} = -eZ_{d0}$, where Z_{d0} is the dust charge number and $|e|$ is the absolute value of the charge of an electron, since the charge acquired by dust particles via collisional processes is negative. In the derivation of equations (3), it was assumed for simplicity that all dust particles are spherical, with radius a . Details of the derivation of equations (3) can be obtained in Ziebell et al. (2008).

Using the expressions for the components ε_{ij} given by equations (3), the dispersion relation can

be written in a very simple form, depending on the integral quantities $J(s, m, h; f_{\beta 0})$,

$$N_{\parallel}^2 = 1 + \frac{1}{2z^2} \sum_{\beta} \frac{\omega_{p\beta}^2}{\Omega_i^2} \frac{1}{n_{\beta 0}} J(s, 1, 0; f_{\beta 0}) \quad (5)$$

with $s = \pm 1$. The dependence of the dispersion relation on the velocity distribution functions of the plasma particles appears only in the integral quantities $J(s, m, h; f_{\beta 0})$. For evaluation of these integral quantities, we utilize an approximation, which is to use the average value of the inelastic collision frequency, obtained as follows,

$$\nu_{\beta} \equiv \frac{1}{n_{\beta 0}} \int d^3u \nu_{\beta d}^0(u) f_{\beta 0}(u), \quad (6)$$

instead of the velocity dependent form $\nu_{\beta d}^0(u)$.

For description of the plasma particles, we consider that their velocity distributions can be either PBK distributions or bi-Maxwellian distributions. The PBK distribution to be used is based on the kappa distribution as defined in [Leubner \(2002\)](#), and can be written as follows,

$$\begin{aligned} f_{\beta, \kappa}(u_{\parallel}, u_{\perp}) &= \frac{n_{\beta 0}}{\pi^{3/2} \kappa_{\beta \perp} \kappa_{\beta \parallel}^{1/2} u_{\beta \perp}^2 u_{\beta \parallel}} \\ &\times \frac{\Gamma(\kappa_{\beta \perp}) \Gamma(\kappa_{\beta \parallel})}{\Gamma(\kappa_{\beta \perp} - 1) \Gamma(\kappa_{\beta \parallel} - 1/2)} \\ &\times \left(1 + \frac{u_{\perp}^2}{\kappa_{\beta \perp} u_{\beta \perp}^2}\right)^{-\kappa_{\beta \perp}} \left(1 + \frac{u_{\parallel}^2}{\kappa_{\beta \parallel} u_{\beta \parallel}^2}\right)^{-\kappa_{\beta \parallel}}, \end{aligned} \quad (7)$$

while the bi-Maxwellian velocity distribution is given in dimensionless variables by the well known expression,

$$f_{\beta M}(u_{\parallel}, u_{\perp}) = \frac{n_{\beta 0}}{\pi^{3/2} u_{\beta \perp}^2 u_{\beta \parallel}} e^{-u_{\perp}^2/u_{\beta \perp}^2} e^{-u_{\parallel}^2/u_{\beta \parallel}^2} \quad (8)$$

In equation (7), and in equation (8) as well, we have used the non dimensional thermal velocities for particles of species β , defined as

$$u_{\beta \perp}^2 = \frac{2T_{\beta \perp}}{m_{\beta} v_A^2}, \quad u_{\beta \parallel}^2 = \frac{2T_{\beta \parallel}}{m_{\beta} v_A^2},$$

where $T_{\beta \perp}$ and $T_{\beta \parallel}$ denote respectively the perpendicular and parallel temperatures for particles of species β . The anisotropy of temperatures for a given species is usually denoted by the ratio $T_{\beta \perp}/T_{\beta \parallel}$.

Equation (7) is the form of PBK distribution which has been used in a previous study made on the EMIC instability for dustless plasmas ([dos Santos et al. 2015](#)), and also in studies made on waves in the whistler branch, in dustless and in dusty plasmas ([dos Santos et al. 2014, 2016](#)), respectively.

As can be easily verified from equation (7), a PBK distribution has two sources of anisotropy between perpendicular and parallel directions, the difference in the temperature variables $T_{\beta \perp}$ and $T_{\beta \parallel}$, and the difference in the kappa indexes $\kappa_{\beta \perp}$ and $\kappa_{\beta \parallel}$. Effective temperatures along perpendicular and parallel directions can be defined, and in energy units are given as follows,

$$\theta_{\beta \perp} = m_{\beta} \int d^3v \frac{v_{\perp}^2}{2} f_{\beta 0} = \frac{\kappa_{\beta \perp}}{\kappa_{\beta \perp} - 2} T_{\beta \perp}, \quad (9)$$

$$\theta_{\beta \parallel} = m_{\beta} \int d^3v v_{\parallel}^2 f_{\beta 0} = \frac{\kappa_{\parallel}}{(\kappa_{\parallel} - 3/2)} T_{\beta \parallel}.$$

It is seen that the effective temperatures $\theta_{\beta \perp}$ and $\theta_{\beta \parallel}$ are larger than the corresponding temperatures $T_{\beta \perp}$ and $T_{\beta \parallel}$. This feature is characteristic of distributions based on the kappa distribution as defined in [Leubner 2002](#). Kappa distributions as defined in [Summers and Thorne \(1991\)](#), which are not considered in the present paper, feature effective temperatures which are equal to the respective temperatures $T_{\beta \perp}$ and $T_{\beta \parallel}$ ([Livadiotis and McComas 2013b,a; Livadiotis 2015](#)).

Using $f_{\beta 0}$ as the distribution given by equation (7), with use of the approximation given by equation (6), the integral J appearing in the dispersion relation, given by equation (5), becomes as follows ([Galvão et al. 2011](#))

$$\begin{aligned} J(s, 1, 0; f_{\beta 0}) &= n_{\beta 0} \frac{2\kappa_{\beta \perp}}{\kappa_{\beta \perp} - 2} \left[-\frac{\kappa_{\beta \perp} - 2}{\kappa_{\beta \perp}} \right. \\ &+ \frac{u_{\beta \perp}^2}{u_{\beta \parallel}^2} \frac{\kappa_{\beta \parallel} - 1/2}{\kappa_{\beta \parallel}} + \left(\zeta_{\beta}^0 - \hat{\zeta}_{\beta}^s \right) \frac{\kappa_{\beta \perp} - 2}{\kappa_{\beta \perp}} Z_{\kappa_{\beta \parallel}}^{(0)}(\zeta_{\beta}^s) \\ &\left. + \frac{u_{\beta \perp}^2}{u_{\beta \parallel}^2} \zeta_{\beta}^s Z_{\kappa_{\beta \parallel}}^{(1)}(\zeta_{\beta}^s) \right], \end{aligned} \quad (10)$$

where

$$\zeta_{\beta}^0 = \frac{z}{q_{\parallel} u_{\beta \parallel}}, \quad \zeta_{\beta}^s = \frac{z - sr_{\beta} + i\tilde{\nu}_{\beta}}{q_{\parallel} u_{\beta \parallel}}, \quad (11)$$

$$Z_{\kappa_{\beta \parallel}}^{(0)}(\xi) = i \frac{\kappa_{\beta \parallel} - 1/2}{\kappa_{\beta \parallel}^{3/2}} \quad (12)$$

$$\begin{aligned}
& \times {}_2F_1 \left[1, 2\kappa_{\beta\parallel}, \kappa_{\beta\parallel} + 1; \frac{1}{2} \left(1 + \frac{i\xi}{\kappa_{\beta\parallel}^{1/2}} \right) \right], \\
& \kappa_{\beta\parallel} > -1/2 \\
Z_{\kappa_{\beta\parallel}}^{(1)}(\xi) &= i \frac{(\kappa_{\beta\parallel} - 1/2)(\kappa_{\beta\parallel} + 1/2)}{\kappa_{\beta\parallel}^{3/2}(\kappa_{\beta\parallel} + 1)} \quad (13) \\
& \times {}_2F_1 \left[1, 2\kappa_{\beta\parallel} + 2, \kappa_{\beta\parallel} + 2; \frac{1}{2} \left(1 + \frac{i\xi}{\kappa_{\beta\parallel}^{1/2}} \right) \right], \\
& \kappa_{\beta\parallel} > -3/2,
\end{aligned}$$

and where ${}_2F_1$ is the hypergeometric Gauss function.

Using $f_{\beta 0}$ as the bi-Maxwellian distribution function given by equation (8), and using the approximation given by equation (6), the J integral which has to be used in the dispersion relation becomes the following

$$\begin{aligned}
J(s, 1, 0; f_{\beta 0}) &= 2n_{\beta 0} \left\{ \zeta_{\beta}^0 Z(\zeta_{\beta}^n) \right. \quad (14) \\
& \left. - \left(1 - \frac{u_{\beta\perp}^2}{u_{\beta\parallel}^2} \right) [1 + \zeta_{\beta}^n Z(\zeta_{\beta}^n)] \right\},
\end{aligned}$$

where Z is the well-known plasma dispersion function (Fried and Conte 1961),

$$Z(\zeta) = \frac{1}{\sqrt{\pi}} \int_{-\infty}^{+\infty} dt \frac{e^{-t^2}}{t - \zeta} \quad (15)$$

A timely comment is that equation (10), for $\kappa_{\beta\parallel} \rightarrow \infty$ and $\kappa_{\beta\perp} \rightarrow \infty$, becomes the same as equation (14).

3. Numerical Analysis

For the numerical analysis about the effect of dust on the dispersion relation of IC waves, and on the growth rate of the EMIC instability, we consider the same parameters which we have used in our previous study about the IC waves, which was made without considering the presence of dust (dos Santos et al. 2015), and add the dust population. For the non dimensional parameters v_A/c and β_i we assume the values $v_A/c = 1.0 \times 10^{-4}$ and $\beta_i = 2.0$ (except for one figure, where we take $\beta_i = 0.2$), for the ion charge number we

take $Z_i = 1.0$, and for the ion mass we assume $m_i = m_p$, the mass of a proton. Moreover, since we are interested in an instability generated by anisotropy in the ion distribution, we consider in all cases to be studied that the electron temperature is isotropic and is the same as the ion parallel temperature, $T_e = T_{i\parallel}$. With this choice of parameters, the results to be obtained in the present analysis, in the limit of vanishing dust population, can be directly compared with the results obtained in dos Santos et al. (2015). When a dust population is taken into account, we assume micrometric particles, with radius $a = 1.0 \times 10^{-4}$ cm. Moreover, in the ensuing numerical analysis, the number density of the dust population is given in terms of the number density of the ion population, which is another parameter which has to be assumed. We take the ion number density as $n_{i0} = 1.0 \times 10^9 \text{ cm}^{-3}$, value which can be representative of outbursts in carbon-rich stars, environment where effects associated to the presence of dust are expected to be very significant (Tsytovich et al. 2004). In fact, it was even argued that in these environments the conditions may be such that dust grains can eventually become coupled, forming dust molecules (Tsytovich et al. 2004). Such strongly coupled dusty plasmas are not contemplated in our analysis, which is valid for weakly coupled dust. With the choice made for the ion number density, the results to be obtained in the present analysis can be compared, in the limit where the particle distributions tend to be Maxwellian or bi-Maxwellian, with results obtained in de Juli et al. (2007), where the same set of parameters has been utilized.

Using these parameters, we solve the dispersion relation considering different forms of the distribution functions for ions and electrons, and different values of the number density population of dust particles. Initially, we consider the effects of the presence of the dust on the imaginary part of the frequency, which can be appreciated in figure 1, where the results obtained in the case without the presence of dust are shown at the left side column, and the results obtained in the presence of a small population of dust appear at the right side column. In figure 1 we consider the case of a small population of dust, with relative number density $\epsilon = n_{d0}/n_{i0} = 2.5 \times 10^{-6}$, where n_{d0} is the equilibrium values of the dust number density.

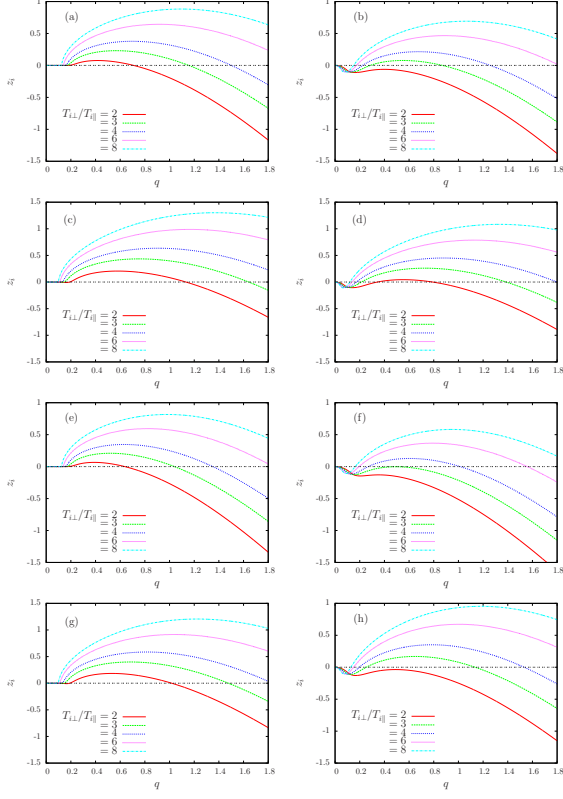


Fig. 1.— Imaginary part of the normalized frequency of waves in the IC mode (z_i) vs. normalized wave number q , for different forms of ion and electron distribution functions, and different values of the ion temperature ratio ($T_{i\perp}/T_{i\parallel} = 2, 3, 4, 6$, and 8). At the left column, $\epsilon = 0$; at the right column, $\epsilon = 2.5 \times 10^{-6}$. The plasma parameters are $\beta_i = 2.0$, $v_A/c = 1.0 \times 10^{-4}$, $n_{i0} = 1.0 \times 10^9 \text{ cm}^{-3}$, and $a = 1.0 \times 10^{-4} \text{ cm}$, with isotropic electron temperature, $T_e = T_{i\parallel}$. (a) and (b) Bi-Maxwellian distribution for ions and isotropic Maxwellian for electrons; (c) and (d) PBK distribution with $\kappa_{i\perp} = \kappa_{i\parallel} = 5$ for ions, and isotropic Maxwellian for electrons; (e) and (f) Bi-Maxwellian distribution for ions and PBK distribution for electrons, with $\kappa_{e\perp} = \kappa_{e\parallel} = 5$; (g) and (h) PBK distribution with $\kappa_{i\perp} = \kappa_{i\parallel} = 5$ for ions and PBK distribution for electrons, with $\kappa_{e\perp} = \kappa_{e\parallel} = 5$.

The individual curves show the results obtained considering different values of the ion temperature anisotropy, $T_{i\perp}/T_{i\parallel} = 2, 3, 4, 6$, and 8 . Figures 1(a) and 1(b) show the results obtained considering for the ions a bi-Maxwellian distribution and for the electrons an isotropic Maxwellian distribution, so that for both species the integral J in the dispersion relation (5) is given by equation (14). It is seen that the growth rates of the instability, that is, the magnitude of the values of $z_i > 0$, increase with the increase of the temperature ratio, both in the case without dust and in the case with dust. It is also seen that the range of values of q where instability occurs increases as well. The effect of the presence of a small population of dust is seen in the comparison between figures 1(a), no dust, and 1(b), with case. Figure 1(b) features a slight overall reduction of $|z_i|$, in comparison with figure 1(a), and also show the occurrence of a region of damping rates ($z_i < 0$) for small values of q , which is not seen in figure 1(a).

In the case depicted in figures 1(c) and 1(d) the electron distribution is the same as in panels (a) and (b), but for the ions we have a PBK distribution as given by equation (7), with $\kappa_{i\perp} = \kappa_{i\parallel} = 5.0$ and the same values of ion temperature ratios as in figures 1(a) and 1(b), and also the same values for the other parameters. With this combination of distribution functions, the electron contribution to the dispersion relation contains J as given by equation (14), and the ion contribution contains J as given by equation (10). The comparison between figures 1(c) and 1(a), both obtained without dust, shows that the increase in the non thermal character of the ion distribution, due to the use of the PBK distribution, contributes to increase the instability both in magnitude of the growth rates and in the range of wave numbers with instability. The comparison between figures 1(c) and 1(d) shows that in this case the effect of the presence of a small population of the dust is similar to that seen in the case of ions with bi-Maxwellian distribution, in figures 1(a) and 1(b). The presence of the dust population leads to small reduction of the magnitude of the values of $|z_i|$, decrease of the range of unstable wave numbers, and occurrence of a damping region for small values of q .

Figures 1(e) and 1(f) show the case of ions with bi-Maxwellian distributions and electrons with isotropic PBK distribution, assuming $\kappa_{e\perp} =$

$\kappa_{e\parallel} = 5.0$, with ion temperature ratios and other parameters as in figures 1(a) and 1(b). The only difference between panels (e) and (f) and panels (a) and (b), respectively, is the electron distribution function. Figures 1(e) and 1(f) show that in the case of PBK distribution for electrons the magnitude of the values of z_i and the range of values of q with positive z_i are reduced compared to the case of Maxwellian electron distribution seen in panels (a) and (b). This observation was also made in the case of ion firehose instability, both in a plasma without dust (dos Santos et al. 2014) and in a plasma with a dust population (dos Santos et al. 2016). The effect of the presence of the dust is a slight reduction of the growth rates and of the range of unstable wave numbers, seen in the comparison between figures 1(f) and 1(e).

The final panels of figure 1 are panels (g) and (h), which show results obtained considering PBK distributions for both ions and electrons, with $\kappa_{e\perp} = \kappa_{e\parallel} = 5.0$ and $\kappa_{i\perp} = \kappa_{i\parallel} = 5.0$, with the same parameters and ion temperature ratios as in panels (a) and (b). It is seen that the values of z_i are larger in panels (g) and (h) than in panels (a) and (b), respectively, indicating dominance of the influence of the non thermal character of the ion distribution over the effect of the non thermal character of the electron distribution. That is, for the same kappa indexes, the tendency to increase the instability, caused by the PBK ion distribution, is seen to be more significant than the tendency of decrease in the instability, associated to the PBK electron distribution. The effect of the presence of a small population of dust is similar to the effect seen in the case of the other combinations of ion and electron distribution functions, with the appearing of a region with damping for small q and small decrease of the growth rates and of the range of wave numbers with instability.

Figure 2 presents the values of the real part of the roots of the dispersion relation, z_r , corresponding to the imaginary parts appearing in figure 1. The sequence of panels from top to bottom of figure 1 shows that the modification in the ion or electron distribution functions, from Maxwellian to PBK with relatively small value of the kappa indexes, produces some quantitative change in the values of z_r , but does not modify the quantitative dependence on normalized wave number q , or on the ion temperature ratios.

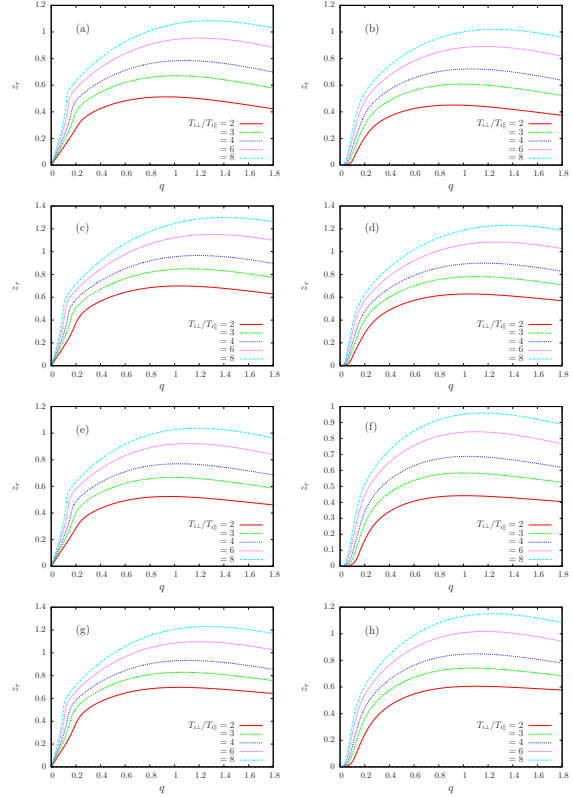


Fig. 2.— Real part of the normalized frequency of waves in the IC mode (z_r) vs. normalized wave number q , for different forms of ion and electron distribution functions, and different values of the ion temperature ratio ($T_{i\perp}/T_{i\parallel} = 2, 3, 4, 6$, and 8). At the left column, $\epsilon = 0$; at the right column, $\epsilon = 2.5 \times 10^{-6}$. The plasma parameters are the same as in figure 1. (a) and (b) Bi-Maxwellian distribution for ions and isotropic Maxwellian for electrons; (c) and (d) PBK distribution with $\kappa_{i\perp} = \kappa_{i\parallel} = 5$ for ions, and isotropic Maxwellian for electrons; (e) and (f) Bi-Maxwellian distribution for ions and PBK distribution for electrons, with $\kappa_{e\perp} = \kappa_{e\parallel} = 5$; (g) and (h) PBK distribution with $\kappa_{i\perp} = \kappa_{i\parallel} = 5$ for ions and PBK distribution for electrons, with $\kappa_{e\perp} = \kappa_{e\parallel} = 5$.

In figure 3 we present the values of the imaginary and real parts of the roots of the dispersion relation for IC waves, considering fixed value of the ion temperature ratio, different forms of the velocity distribution functions, and different values of the dust density. The panels at the left column show the values of z_i , while the panels at the right column show the corresponding values of z_r . We consider temperature ratio $T_{i\perp}/T_{i\parallel} = 5.0$, five values of dust density, and other parameters as in figure 1. The sequence of figures at the left column, from top to bottom, show that the overall effect of the presence of dust is a reduction of the instability, both in the magnitude of the growth rates as in the range of unstable wave numbers. However, the effectiveness of the influence of the dust depends upon the velocity distribution functions. In the case of electrons with Maxwellian distribution and ions bi-Maxwellian distribution, shown in figures 3(a) and 3(b), the EMIC instability ceases to exist for dust population with number density slightly above $\epsilon = 7.5 \times 10^{-6}$. If the ion distribution is modified to be a PBK distribution, with $\kappa_{i\perp} = \kappa_{i\parallel} = 5.0$, the instability only disappears if the relative number density of the dust population is above $\epsilon = 1.0 \times 10^{-5}$, as seen in figure 3(c). On the other hand, if the ion distribution is bi-Maxwellian and the electron distribution is a PBK distribution with $\kappa_{e\perp} = \kappa_{e\parallel} = 5.0$, the instability disappears with a dust population with number density $\epsilon \simeq 5.0 \times 10^{-6}$, as seen in figure 3(e). In the panel at the left column of the last line, 3(g), obtained assuming that both ions and electrons are described by PBK distributions, it is seen that the instability disappears for $\epsilon \simeq 9.0 \times 10^{-6}$, a value which is intermediate between the values obtained in the cases of figures 3(c) and 3(e).

In figure 4 we investigate the effect of the value of the kappa index on the EMIC instability, when ions and/or electrons are described by PBK distributions. The left column shows the values of the imaginary parts z_i and the right column shows the values of the real parts z_r , obtained from numerical solution of the dispersion relation. For all panels of figure 4, we consider fixed values of ion temperature ratio, $T_{i\perp}/T_{i\parallel} = 5.0$, and dust relative number density, $\epsilon = 2.5 \times 10^{-6}$, with other parameters the same as those used in the case of figure 1. In figures 4(a) and 4(b) we show results obtained in the case that the electrons are de-

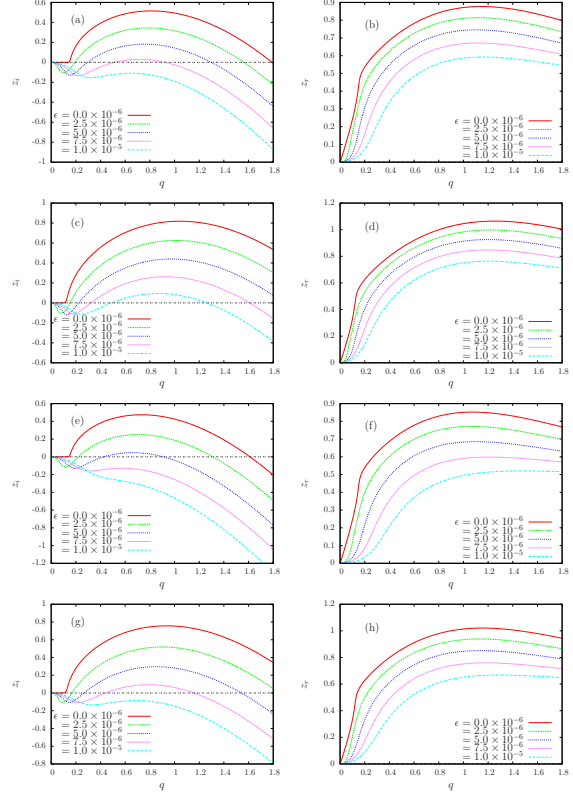


Fig. 3.— Imaginary part (z_i , left column) and real part (z_r , right column), of the normalized frequency for IC mode waves, vs. normalized wave number q , for different forms of ion and electron distribution functions, and different values of the dust density ratio ($\epsilon = 0, 2.5 \times 10^{-6}, 5.0 \times 10^{-6}, 7.5 \times 10^{-6}$, and 1.0×10^{-5}). Parameters are $T_{i\perp}/T_{i\parallel} = 5.0$, and other parameters as in figure 1. (a) and (b) Bi-Maxwellian distribution for ions and isotropic Maxwellian for electrons; (c) and (d) PBK distribution with $\kappa_{i\perp} = \kappa_{i\parallel} = 5$ for ions, and isotropic Maxwellian for electrons; (e) and (f) Bi-Maxwellian distribution for ions and PBK distribution for electrons, with $\kappa_{e\perp} = \kappa_{e\parallel} = 5$; (g) and (h) PBK distribution with $\kappa_{i\perp} = \kappa_{i\parallel} = 5$ for ions and PBK distribution for electrons, with $\kappa_{e\perp} = \kappa_{e\parallel} = 5$.

scribed by a Maxwellian distribution, and the ions are described by a PBK distribution, considering five values of the kappa indexes, $\kappa_{i\perp} = \kappa_{i\parallel} = 20, 10, 6, 5,$ and 4 . The ratios of effective temperatures are therefore $\theta_{i\perp}/\theta_{i\parallel} = 5.14, 5.31, 5.63, 5.83,$ and 6.25 , respectively. Figure 4(a) shows that for κ_i indexes equal to 20, the EMIC instability occurs for $0.2 \leq q \leq 1.65$. With decrease of the kappa indexes to 10, the upper limit of the unstable region is moved to $q \simeq 1.8$, and the lower limit is decreased from the previous value. With further decrease of the kappa indexes, the unstable region increases considerably, extending well beyond the maximum value of q which is shown in figure 3. The lower limit of the unstable region continues to decrease, being $q \simeq 0.13$ for kappa indexes equal to 4. The maximum value of the growth rate also increases with the decrease of the ion kappa indexes, being $z_i \simeq 0.38$ at $q \simeq 0.8$, in the case of $\kappa_{i\perp} = \kappa_{i\parallel} = 20$, and $z_i \simeq 0.77$ at $q \simeq 1.1$, in the case of $\kappa_{i\perp} = \kappa_{i\parallel} = 4$.

In figure 4(c) and 4(d) we present results obtained from numerical solution of the dispersion relation in the case of ions described by a bi-Maxwellian distribution and electrons described by PBK distribution, with $\kappa_{e\perp} = \kappa_{e\parallel} = 20, 10, 6, 5,$ and 4 . Despite the isotropy of electron temperature, $T_{e\perp} = T_{e\parallel}$, there is an effective electron anisotropy given by $\theta_{e\perp}/\theta_{e\parallel}$, which goes from 1.03 in the case of kappa indexes equal to 20, to 1.25 in the case of kappa indexes equal to 4. Figure 4(c) shows that the decrease of the kappa indexes of the electron distribution is associated to decrease in the magnitude of the growth rates and range of the EMIC instability, contrarily to what was observed in the case of decrease of the kappa indexes of the ion distribution, in figure 4(a). For the real part of the dispersion relation, figure 4(d) shows that the effect of the kappa index in the electron distribution is very small, much less significant than the effect due to the ion kappa indexes, seen in figure 4(a).

In figure 4(e) and 4(f) we depict results obtained considering both ions and electrons described by PBK distributions, with the same kappa indexes, considering kappa indexes 20, 10, 6, 5, and 4. In consonance with the results shown in figures 4(a) and 4(c), where it is seen that the growth rate of the EMIC instability tends to increase with the decrease of the kappa index in

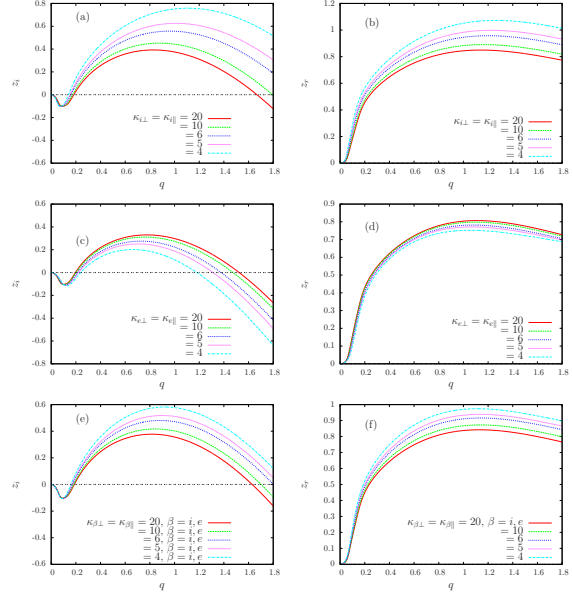


Fig. 4.— Imaginary part (z_i , left column) and real part (z_r , right column), of the normalized frequency for IC mode waves, vs. normalized wave number q , for different forms of ion and electron distribution functions, with several values of the kappa index. Parameters are $\beta_i = 2.0$, $v_A/c = 1.0 \times 10^{-4}$, $n_{i0} = 1.0 \times 10^9 \text{ cm}^{-3}$, $T_{i\perp}/T_{i\parallel} = 5.0$, $a = 1.0 \times 10^{-4} \text{ cm}$, $\epsilon = 2.5 \times 10^{-6}$, with isotropic electron temperature, $T_e = T_{i\parallel}$. (a) and (b) PBK distribution with $\kappa_{i\perp} = \kappa_{i\parallel}$ for ions, with κ values 20, 10, 6, 5, and 4, and Maxwellian distribution for electrons; (c) and (d) Bi-Maxwellian distribution for ions and PBK distribution for electrons, with $\kappa_{e\perp} = \kappa_{e\parallel}$, with κ values 20, 10, 6, 5, and 4; (e) and (f) PBK distribution with $\kappa_{i\perp} = \kappa_{i\parallel} = 5$ for ions and PBK distribution for electrons, with $\kappa_{e\perp} = \kappa_{e\parallel}$, and κ values 20, 10, 6, 5, and 4.

the ion PBK distribution, and decrease with the decrease of the kappa index in the electron PBK distribution, the results shown in figure 4(e) feature growth rates with values which are in between those obtained in panels (a) and (c). For instance, in the case of kappa values equal to 5, figure 4(e) shows that the maximum value of z_i is nearly 0.51, while it is $z_i \simeq 0.6$ in the case of figure 4(a) and $z_i \simeq 0.23$ in figure 4(c).

Figure 5 reproduces the analysis made in figure 3, but considering $\beta_i = 0.2$ (i.e., a small-beta plasma), instead of $\beta = 2.0$. As in the case presented in figure 3, the panels which constitute figure 5, from top to bottom, show that the presence of dust leads to a reduction of the instability, both in magnitude of the growth rates and in the range of unstable wave numbers, with effectiveness which depends upon the velocity distribution functions. In the case of electrons with Maxwellian distribution and ions bi-Maxwellian distribution, shown in figures 5(a) and 5(b), the EMIC instability ceases to exist for $\epsilon \simeq 6.0 \times 10^{-6}$. Figures 5(c) and 5(d) show the case of PBK ion distribution and Maxwellian electron distribution, with $\kappa_{i\perp} = \kappa_{i\parallel} = 5.0$, and it is seen that the instability only disappears if the relative number density of the dust population is near $\epsilon = 1.0 \times 10^{-5}$. If the ion distribution is bi-Maxwellian and the electrons have a PBK distribution with $\kappa_{e\perp} = \kappa_{e\parallel} = 5.0$, the instability disappears for $\epsilon \simeq 5.0 \times 10^{-6}$, as seen in figure 5(e). Figure 5(g) shows that, when both ions and electrons are described by PBK distributions, with the same kappa indexes, the instability disappears for $\epsilon \simeq 7.5 \times 10^{-6}$, a value which is intermediate between the values obtained in the cases of figures 5(c) and 5(e). The comparison between the results displayed at the left column of figure 5 and the results depicted at the left column in figure 3, show that despite the fact that range in wavenumber of the EMIC tend to decrease with the decrease of β_i , the effects of the presence of dust on the growth rate tend to remain qualitatively similar. On the other hand, the comparison between the right columns of figures 5 and 3, indicate that the effect of the dust on the real part of the dispersion relation decreases with the decrease of β_i , for all the combinations of ion and electron distribution functions which have been considered.

In figures 6 and 7 we investigate the effect of anisotropy of the κ indexes in the ion distribu-

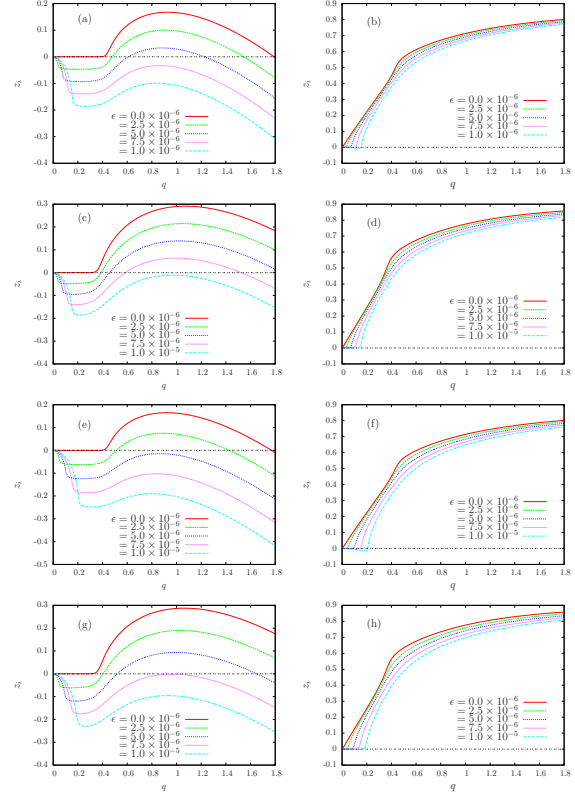


Fig. 5.— Imaginary part (z_i , left column) and real part (z_r , right column), of the normalized frequency for IC mode waves, vs. normalized wave number q , for different forms of ion and electron distribution functions, and different values of the dust density ratio ($\epsilon = 0, 2.5 \times 10^{-6}, 5.0 \times 10^{-6}, 7.5 \times 10^{-6}$, and 1.0×10^{-5}). The plasma parameters are $\beta_i = 0.2$, $v_A/c = 1.0 \times 10^{-4}$, $n_{i0} = 1.0 \times 10^9 \text{ cm}^{-3}$, and $a = 1.0 \times 10^{-4} \text{ cm}$, with isotropic electron temperature, $T_e = T_{i\parallel}$, and with $T_{i\perp}/T_{i\parallel} = 5.0$. (a) and (b) Bi-Maxwellian distribution for ions and isotropic Maxwellian for electrons; (c) and (d) PBK distribution with $\kappa_{i\perp} = \kappa_{i\parallel} = 5$ for ions, and isotropic Maxwellian for electrons; (e) and (f) Bi-Maxwellian distribution for ions and PBK distribution for electrons, with $\kappa_{e\perp} = \kappa_{e\parallel} = 5$; (g) and (h) PBK distribution with $\kappa_{i\perp} = \kappa_{i\parallel} = 5$ for ions and PBK distribution for electrons, with $\kappa_{e\perp} = \kappa_{e\parallel} = 5$.

tion, considering isotropic electron and ion temperatures. The column at the left show the values of z_i , and the right column show the values of z_r .

In the case of figure 6, we consider a fixed value of the relative dust density, $\epsilon = 2.5 \times 10^{-6}$, and other parameters as in figure 1. For this figure, we assume PBK ion distributions, with isotropic temperatures, $\kappa_{i\parallel} = 30$, and four values of $\kappa_{i\perp}$, namely $\kappa_{i\perp} = 20, 10, 5$, and 2.93 . These values of the ion kappa parameters correspond to effective ion temperature ratio given by $1.06, 1.19, 1.58$, and 2.99 , respectively. Panels (a) and (b) depict results obtained considering isotropic Maxwellian distribution for electrons, and panels (c) and (d) show results obtained considering PBK distribution for electrons, with $\kappa_{e\perp} = \kappa_{e\parallel} = 5.0$, and isotropic temperatures. We can compare the results appearing in figure 6(a) with those in figure 1(d), which was obtained considering the same parameters and similar combination of velocity distribution functions, except that in figure 1(d) the ion kappa indexes were isotropic and the ion temperatures were anisotropic. For instance, it is seen in figure 1(d) that for $T_{i\perp}/T_{i\parallel} = 3.0$ there is instability in the range $0.2 \leq q \leq 1.4$, with maximum value $z_i \simeq 0.25$. In the case of figure 6(a) the instability which appears for $\kappa_{i\perp} = 2.93$ ($\theta_{i\perp}/\theta_{i\parallel} = 2.99$) occurs for $0.3 \leq q \leq 0.9$, with smaller value of the maximum growth rate. Another comparison which can be made is between the growth rates appearing in figures 6(c) and 1(h). Both figures show results obtained with PBK distributions for ions and electrons, with anisotropic temperatures in figure 1 and anisotropic ion kappa indexes in figure 6. In figure 1(h) the instability for $T_{i\perp}/T_{i\parallel} = 3.0$ occurs in the region $0.22 \leq q \leq 1.15$, with maximum growth rate which approaches $z_i = 0.2$. In figure 6(c), the case with $\kappa_{i\perp} = 2.93$, for which the ratio of effective temperature is $\theta_{i\perp}/\theta_{i\parallel} = 2.99$, does not show positive values of z_i . The conclusion which can be drawn is that the anisotropy in the effective temperature which is due to the anisotropy of the kappa parameters of the ion distribution is not so effective as the anisotropy of the ion temperature parameters, on the effectiveness of the EMIC instability.

In figure 7 we investigate with more detail the role of the dust density in the case of ions with a PBK distribution, considering several values of the dust relative density, and other parameters which

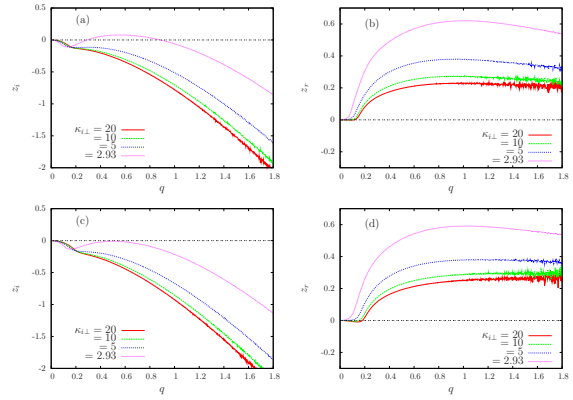


Fig. 6.— Imaginary part (z_i , left column) and real part (z_r , right column), of the normalized frequency for IC mode waves, vs. normalized wave number q , for different forms of ion and electron distribution functions, with isotropic ion temperatures and different values of anisotropy in the ion kappa indexes. Parameters are $\beta_i = 2.0$, $v_A/c = 1.0 \times 10^{-4}$, $n_{i0} = 1.0 \times 10^9 \text{ cm}^{-3}$, $a = 1.0 \times 10^{-4} \text{ cm}$, $\epsilon = 2.5 \times 10^{-6}$, and isotropic electron temperature $T_e = T_{i\parallel}$. (a) and (b) PBK distribution for ions, with $\kappa_{i\parallel} = 30$ and several values of $\kappa_{i\perp}$ (20, 10, 5, and 2.93), and isotropic Maxwellian for electrons; (c) and (d) PBK distribution for ions, with $\kappa_{i\parallel} = 30$ and several values of $\kappa_{i\perp}$ (20, 10, 5, and 2.93), and PBK distribution for electrons, with $\kappa_{e\parallel} = \kappa_{e\perp} = 5.0$.

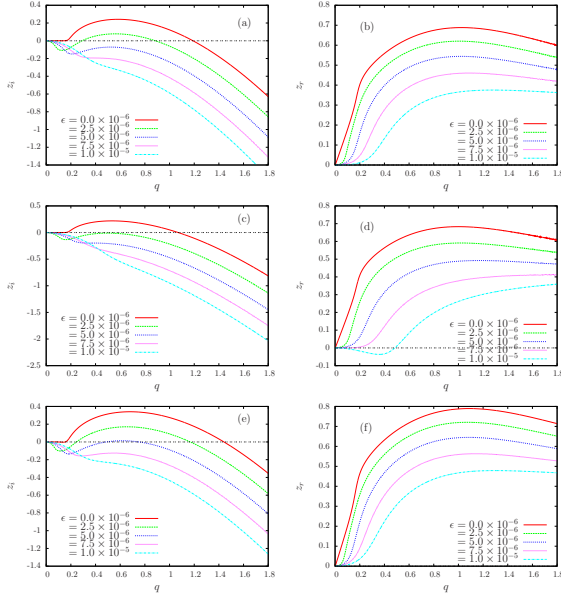


Fig. 7.— Imaginary part (z_i , left column) and real part (z_r , right column), of the normalized frequency for IC mode waves, vs. normalized wave number q , for different forms of ion and electron distribution functions, and several values of the relative dust number density ($\epsilon = 0, 2.5 \times 10^{-6}, 5.0 \times 10^{-6}, 7.5 \times 10^{-6}$, and 1.0×10^{-5}). Other parameters are $\beta_i = 2.0$, $v_A/c = 1.0 \times 10^{-4}$, $n_{i0} = 1.0 \times 10^9 \text{ cm}^{-3}$, $a = 1.0 \times 10^{-4} \text{ cm}$, and isotropic electron temperature $T_e = T_{i\parallel}$. (a) and (b) PBK distribution for ions, with $\kappa_{i\parallel} = 30$ and $\kappa_{i\perp} = 2.93$, with $T_{i\perp} = T_{i\parallel}$, and isotropic Maxwellian for electrons; (c) and (d) PBK distribution for ions, with $\kappa_{i\parallel} = 30$ and $\kappa_{i\perp} = 2.93$, with $T_{i\perp} = T_{i\parallel}$, and PBK distribution for electrons, with $\kappa_{e\parallel} = \kappa_{e\perp} = 5.0$; (e) and (f) PBK distribution for ions, with $\kappa_{i\parallel} = \kappa_{i\perp} = 5.0$ and $T_{i\perp}/T_{i\parallel} = 2.565$, and isotropic Maxwellian for electrons.

are the same as in the case of figure 1. As in previous figures, the left column shows the values of z_i and the right column shows the values of z_r . Figures 7(a) and (b) show results obtained assuming a PBK ion distributions with isotropic temperatures and anisotropic kappa parameters, with an isotropic Maxwellian to describe the electron population. The ion kappa parameters are $\kappa_{i\parallel} = 30$ and $\kappa_{i\perp} = 2.93$, so that the effective temperature anisotropy of the ion distribution is $\theta_{i\perp}/\theta_{i\parallel} = 2.99$. For this case, the values of z_i seen in figure 7(a) show that the EMIC instability disappears for dust population between the values $\epsilon = 2.5 \times 10^{-6}$ and $\epsilon = 5.0 \times 10^{-6}$. Figures 7(c) and 7(d) show results obtained assuming that the electron distribution function is a PBK distribution, with isotropic temperatures and $\kappa_{e\parallel} = \kappa_{e\perp} = 5.0$, instead of an isotropic Maxwellian, with the ion distribution and other parameters equal to those used in the case shown in figures 7(a) and 7(b). This example shows that, also in the case of ion distribution with anisotropy due to the kappa indexes, the increase of the non thermal character of the electron distribution, with the presence of a power-law electron tail, contributes to decrease the EMIC instability due to the anisotropic ion distribution.

For comparison with the results shown in figure 7(a), figure 7(e) shows the values of z_i obtained with isotropic Maxwellian distribution for electrons and PBK distribution for ions, with isotropic ion kappa indexes $\kappa_{i\perp} = \kappa_{i\parallel} = 5.0$ and anisotropy due to the ion temperatures. We choose the ion temperature ratio as $T_{i\perp}/T_{i\parallel} = 2.565$, which leads to the same anisotropy of the effective temperatures as in figure 7(a). It is seen that in the case of figure 7(e) the instability is slightly stronger, with larger range of unstable wave numbers, than in the case of figure 7(a). As already noticed in the commentaries about figure 6, it is seen that the anisotropy which is due to anisotropic kappa indexes is not so effective in producing the EMIC instability as the anisotropy due to the ion temperatures.

4. Conclusions

We have presented results obtained from a numerical analysis of the dispersion relation for low-frequency ion-cyclotron waves propagating along

the ambient magnetic field in a dusty plasma, considering situations where either ions or electrons, or both, have product-bi-kappa velocity distributions. Regarding the influence of the shape of the velocity distribution, results obtained considering absence of dust have shown that, if the electrons are described by an isotropic Maxwellian distribution and the ion distribution is changed from the bi-Maxwellian limit to a PBK distribution with relatively small kappa index, the range in wavenumber where instability occurs is increased, and the magnitude of the growth rates is increased as well. Conversely, if the ion distribution is a bi-Maxwellian distribution and the electron distribution is changed from a Maxwellian distribution into a PBK distribution with small kappa index, with isotropic electron temperature, the magnitude and range of the EMIC instability is very little affected. This weak dependence of the growth rates of the EMIC instability on non thermal features of the electron distribution is in contrast with the dependence reported in the literature in the case of the ion-firehose instability, for which it has been seen that the adoption of a PBK distribution with small kappa index for electrons leads to strong reduction of the instability (dos Santos et al. 2016). Regarding the influence of dust, the results obtained have shown that, for all shapes of ion and electron distributions which have been utilized, the presence of a small population of dust leads to some decrease in the magnitude of the growth rates and in the range of the EMIC instability, in comparison with the case without dust. We have also seen that in presence of dust a region of wave damping appears for small values of q , which is not present in the dustless case. All these features related to different forms of ion and electron distributions, and to the presence of a small amount of dust, have been obtained considering the plasma parameter $\beta_i = 2.0$, and have also been verified considering one example with smaller value of this parameter, $\beta_i = 0.2$.

Still regarding the effect of the presence of dust, the results obtained have shown that a value of the relative number density of dust which is enough to make disappear completely the EMIC instability in bi-Maxwellian plasma, may be not enough to overcome the instability in plasmas with ions described by PBK distributions with small kappa index. It has also been seen that the increase in

the dust population leads to decrease of the phase velocity of the IC waves, for all types of combinations of Maxwellian and PBK distributions which have been investigated.

For fixed temperature ratio $T_{i\perp}/T_{i\parallel}$ and fixed dust number density, it has been seen that the decrease of the kappa index in a PBK ion distribution leads to increase of the instability in range and in magnitude of the growth rate, and that the increase becomes more and more pronounced for progressively smaller ion kappa indexes. On the other hand, for fixed value of $T_{i\perp}/T_{i\parallel}$ and dust density ratio, with bi-Maxwellian distribution for ions, the decrease of the kappa index in a PBK electron distribution leads to decrease of the EMIC instability, in magnitude of the growth rate and in range, but the decrease is not very pronounced.

We have also investigated the effect of anisotropy in the kappa indexes of the ion PBK distribution, for given dust number density and for isotropic ion temperatures. It has been seen that the anisotropy due to the anisotropic kappa indexes is not so effective in producing the EMIC instability as the anisotropy due to the ratio between the ion perpendicular and parallel temperatures.

MSdS acknowledges support from Brazilian agency CAPES. LFZ acknowledges support from CNPq (Brazil), grant No. 304363/2014-6. RG acknowledges support from CNPq (Brazil), grants No. 304461/2012-1 and 478728/2012-3.

REFERENCES

- Andre, N., Ferriere, K.M.: J. Geophys. Res. **113**(A9), 09202 (2008). doi:10.1029/2008JA013179
- Cattaert, T., Hellberg, M.A., Mace, R.L.: Physics Of Plasmas **14**, 082111 (2007)
- de Juli, M.C., Schneider, R.S., Ziebell, L.F., Gaelzer, R.: J. Geophys. Res. **112**, 10105 (2007). doi:10.1029/2007JA012434
- dos Santos, M.S., Ziebell, L.F., Gaelzer, R.: Phys. Plasmas **21**, 112102 (2014). doi:10.1063/1.4900766

- dos Santos, M.S., Ziebell, L.F., Gaelzer, R.: *Phys. Plasmas* **22**, 122107 (2015). doi:10.1063/1.4936972
- dos Santos, M.S., Ziebell, L.F., Gaelzer, R.: *Phys. Plasmas* **23**, 013705 (2016). doi:10.1063/1.4939885
- Fried, B.D., Conte, S.D.: *The Plasma Dispersion Function*. Academic Press, New York (1961)
- Galvão, R.A., Ziebell, L.F., Gaelzer, R., de Juli, M.C.: *Braz. J. Phys.* **41**(4-6), 258 (2011). doi:10.1007/s13538-011-0041-2
- Goertz, C.K.: *Rev. Geophys.* **27**(2), 271 (1989). doi:10.1029/RG027i002p00271
- Grün, E., Zook, H.A., Fechtig, H., Giese, R.H.: *Icarus* **62**(2), 244 (1985). doi:10.1016/0019-1035(85)90121-6
- Grün, E., Krüger, H., Dermott, S., Fectig, H., Graps, A.L., Zook, H.A., Gustafson, B.A., Hamilton, D.P., Hanner, M.S., Heck, A., Horányi, M., Kissel, J., Landblad, B.A., Linkert, D., Linkert, G., Mann, I., McDonnell, J.A.M., Morfill, G.E., Polanskey, C., Schwehm, G., Srama, R.: *Geophys. Res. Lett.* **24**(17), 2171 (1997)
- Hapgood, M., Perry, C., Davies, J., Denton, M.: *Planet. Space Sci.* **59**, 618 (2011). doi:10.1016/j.pss.2010.06.002
- Hellberg, M., Mace, R.: *Phys. Plasmas* **9**(5, 1), 1495 (2002). doi:10.1063/1.1462636
- Imai, M., Lecacheux, A., Moncuquet, M., Bagenal, F., Higgins, C.A., Imai, K., Thieman, J.R.: *J. Geophys. Res.* **120**(3), 1888 (2015). doi:10.1002/2014JA020815
- Ishimoto, H., Mann, I.: *Planet. Space Sci.* **47**(1-2), 225 (1998). doi:10.1016/0019-1035(85)90121-6
- Krueger, H., Strub, P., Gruen, E., Sterken, V.J.: *Astrophys. J.* **812**(2), 139 (2015). doi:10.1088/0004-637X/812/2/139
- Kruger, H., Landgraf, M., Altobelli, N., Grun, E.: *Space Sci. Rev.* **130**(1-4), 401 (2007). doi:10.1016/j.asr.2007.04.066
- Lazar, M.: *Astron. Astrophys.* **547**, 94 (2012). doi:10.1051/0004-6361/201219861
- Lazar, M., Poedts, S.: *Astron. Astrophys.* **494**, 311 (2009a). doi:10.1051/0004-6361:200811109
- Lazar, M., Poedts, S.: *Solar Phys.* **258**, 119 (2009b). doi:10.1007/s11207-009-9405-y
- Lazar, M., Poedts, S.: *Mon. Not. R. Astron. Soc.* **437**(1), 641 (2014). doi:10.1093/mnras/stt1914
- Lazar, M., Poedts, S., Fichtner, H.: *Astron. Astrophys.* **582**, 124 (2015). doi:10.1051/0004-6361/201526509
- Lazar, M., Poedts, S., Schlickeiser, R.: *Astron. Astrophys.* **534**, 116 (2011). doi:10.1051/0004-6361/201116982
- Lazar, M., Schlickeiser, R., Poedts, S.: *Phys. Plasmas* **17**, 062112 (2010). doi:10.1063/1.3446827
- Lazar, M., Pierrard, V., Poedts, S., Schlickeiser, R.: *Astrophys. Space Sci. Proc.* **33**, 97 (2012)
- Leubner, M.P.: *Astrophys. Space Sci.* **282**(3), 573 (2002). doi:10.1023/A:1020990413487
- Livadiotis, G., McComas, D.J.: *Space Sci. Rev.* **175**, 215 (2013a). doi:10.1007/s11214-013-9996-3
- Livadiotis, G., McComas, D.J.: *Space Sci. Rev.* **175**, 183 (2013b). doi:10.1007/s11214-013-9982-9
- Livadiotis, G.: *J. Geophys. Res.* **120**(3), 1607 (2015). doi:10.1002/2014JA020825
- Maksimovic, M., Pierrard, V., Lemaire, J.F.: *Astron. Astrophys.* **324**(2), 725 (1997)
- Maksimovic, M., Zouganelis, I., Chaufray, J.-Y., Issautier, K., Scime, E.E., Littleton, J.E., Marsch, E., McComas, D.J., Salem, C., Lin, R.P., Elliot, H.: *J. Geophys. Res.* **110**, 09104 (2005). doi:10.1029/2005JA011119
- Mann, I.: *Adv. Space Res.* **41**(1), 160 (2008). doi:10.1016/j.asr.2007.04.066
- Mann, I., Kimura, H., Biesecker, D.A., Tsurutani, B.T., Grun, E., McKibben, R.B., Liou, J.C., MacQueen, R.M., Mukai, T., Guhathakurta, M., Lamy, P.: *Space Sci. Rev.* **110**(3-4), 269 (2004). doi:10.1023/B:SPAC.0000023440.82735.ba

- Mann, I.: *Annu. Rev. Astron. Astrophys.* **48**, 173 (2010). doi:10.1146/annurev-astro-081309-130846
- Marsch, E., Ao, X.-Z., Tu, C.-Y.: *J. Geophys. Res.* **109**, 04102 (2004). doi:10.1029/2003JA010330
- Marsch, E.: *Living Rev. Solar Phys.* **3**(1), 1 (2006). cited 19 Sep. 2006, <http://www.livingreviews.org/lrsp-2006-1>. doi:10.12942/lrsp-2006-1
- Mendis, D.A., Horányi, M.: *Rev. Geophys.* **51**(1), 53 (2013). doi:10.1002/rog.20005
- Meyer-Vernet, N., Maksimovic, M., Czechowski, A., Mann, I., Zouganelis, I., Goetz, K., Kaiser, M.L., Cyr, O.C.S., Bougeret, J.-L., Bale, S.D.: *Solar Phys.* **256**(1), 463 (2009). doi:10.1007/s11207-009-9349-2
- Moncuquet, M., Bagenal, F., Meyer-Vernet, N.: *J. Geophys. Res.* **107**(A9), 1260 (2002). doi:10.1029/2001JA900124
- Pierrard, V., Lazar, M.: *Solar Phys.* **267**(1), 153 (2010). doi:10.1007/s11207-010-9640-2
- Pilipp, W., Miggenrieder, H., Montgomery, M., Mühlhäuser, K.-H., Rosenbauer, H., Schwenn, R.: *J. Geophys. Res.* **92**(A2), 1075 (1987a). doi:10.1029/JA092iA02p01075
- Pilipp, W., Miggenrieder, H., Montgomery, M., Mühlhäuser, K.-H., Rosenbauer, H., Schwenn, R.: *J. Geophys. Res.* **92**(A2), 1093 (1987b). doi:10.1029/JA092iA02p01093
- Rao, N.N.: *Phys. Scr.* **48**(3), 363 (1993). doi:10.1088/0031-8949/48/3/015
- Schwenn, R.: *Space Sci. Rev.* **124**, 51 (2006). doi:10.1007/s11214-006-9099-5
- Shukla, P.K.: *Phys. Scr.* **45**, 504 (1992). doi:10.1088/0031-8949/45/5/014
- Summers, D., Thorne, R.M.: *Phys. Fluids B* **3**(8), 1835 (1991). doi:10.1063/1.859653
- Tsytoich, V.N., Morfill, G.E., Thomas, H.: *Plasma Phys. Rep.* **30**(10), 816 (2004). doi:10.1134/1.1809401
- Vasyliunas, V.M.: *J. Geophys. Res.* **73**(9), 2839 (1968). doi:10.1029/JA073i009p02839
- Ziebell, L.F., Schneider, R.S., de Juli, M.C., Gaelzer, R.: *Braz. J. Phys.* **38**(3A), 297 (2008). doi:10.1590/S0103-97332008000300002